Scientia Iranica B (2019) 26(6), 3283–3292

Sharif University of Technology
Scientia Iranica
Transactions B: Mechanical Engineering
http://scientiairanica.sharif.edu

Lattice Boltzmann simulation of blood flow properties and vessel geometry in open and closed vessels: A numerical study

H. Akhtari Shishavan*, I. Mirzaee, and N. Pourmahmoud

Department of Mechanical Engineering, Urmia University, Urmia, Postal Code: 5756151818, Iran.

Received 9 April 2018; received in revised form 10 July 2018; accepted 27 August 2018

KEYWORDS
Lattice Boltzmann method;
Blood flow;
Poiseuille law;
Reynolds number.

Abstract. In the present article, lattice Boltzmann method is utilized to simulate two-dimensional incompressible viscous flow in open and closed microchannels (vessels). The main focus of the present research is to study the physical parameters of blood flow in vessels. The presented computational results are reasonably in agreement with the available data in the literature. In addition, the accuracy of Poiseuille law is investigated for blood flow in the open vessel, too. For this purpose, the effect of the vessel diameter and blood viscosity on blood flow is studied numerically. The obtained results showed that pressure tended to increase the flow, while resistance tends to decrease it. Based on additional results, the effect of blood injection into coronary bifurcation with two closed ends is studied. The blood pressure drop is high at the beginning of the vessel (pressure variation is high between the adjacent points along the vessel); however, after the path along the vessel, the speed of dropping pressure decreases and the pressure difference between the adjoining points decreases along the vessel. Finally, the present results have been compared with the available numerical results that show good agreement.

1. Introduction

In this article, a mesoscopic method under the title of lattice Boltzmann is used. In Lattice Boltzmann Method (LBM), fluid is considered as a cluster of particles, which can collide with each other. This cluster is described in terms of distribution function that can be determined by considering the local average of the microscopic velocities of flow, the local position, and local macroscopic velocity. One of the advantages of this method is its relative simplicity in implementation and compatibility with the desired geometries.

The study of the issues concerning blood flow is one of the most attractive phenomena of physiology. Since blood is considered a non-Newtonian fluid, most of these problems do not have an analytical solution. As a result, numerical simulation can be considered as a useful tool for obtaining a deep and thorough understanding of such phenomena [1]. Blood is a complex fluid made up of different living cells and immersed proteins in plasma fluid. The information related to the velocity profile of blood flow and distribution of shearing stress on small walls of the vessels is quite important for preventing cardiovascular diseases such as atherogenesis and thrombosis [2]. Since red blood cells are small semi-solid particles, they increase blood viscosity and affect the behavior of the fluid. The viscosity of blood is about three times the

*. *Corresponding author.*
E-mail addresses: aktari1362hamed@gmail.com (H. Akhtari Shishavan); i.mirzaee@urmia.ac.ir (I. Mirzaee); n.pormahmod@urmia.ac.ir (N. Pourmahmoud)

doi: 10.24200/sci.2018.50751.1851

viscosity of water. Besides, blood does not present a constant viscosity at all shearing rates. Blood is usually considered as a Newtonian and homogeneous fluid; however, when red blood cells accumulate and make up larger particles, blood exhibits completely non-Newtonian behavior. In addition, the wall pressure and the shear stress of the wall have significant effects on hemodynamics. High levels of shear stress may lead to vascular obstruction and damaging the inner parts of the arteries. Therefore, to understand the physiology of arterial diseases, the study of the hemodynamic factors is important. The most important rheological feature of blood, which has a direct effect on blood movement, is its local viscosity. If the shearing rate is small (lower than 100 s^{-1}), the red cells accumulate and lead to rouleaux. The accumulation of the rouleaux in blood plasma leads to shear-thinning behavior of the blood, which is one of the main reasons for the non-Newtonian behavior of blood flow [3].

Vessel visualization demands a global smooth surface model, which is accurate enough to visually preserve structures of interest [4]. Blood vessel analysis plays a fundamental role in different clinical fields, such as laryngology, oncology, ophthalmology, and neurosurgery [5-9], both for diagnosis, treatment planning, and execution and for treatment outcome evaluation. The importance of vessel analysis is supported by the constant introduction in clinical practice of new medical technologies aimed at enhancing the visualization of vessels, as endoscopy in Narrow Band Imaging (NBI) and cone-beam Computed Tomography (CT) 3D Digital Subtraction Angiography (DSA) [10]. At the same time, standard techniques such as Magnetic Resonance Angiography (MRA) and Computed Tomography Angiography (CTA) are constantly improved to enhance vascular tree visualization [11-13].

Recently, the application of LBM in blood flow has received great attention. The rheology of the red blood cells in micro-canals and their interactive effects on flow have been studied, and the formation of blood clot has been predicted. Besides, blood flow in an artificial heart valve and inside the arteries has been considered. The flow of blood has been simulated in small vessels, too [14]. Of other works in this regard, the study of lattice Boltzmann of the blood flow in a vessel suffering aneurysm using a porous stent can be mentioned, which considers the effect of the stent on the hemodynamic conditions of the flow using the numerical simulation.

The LBM is a useful simulation technique for numerically solving flow problems. This method is also feasible as a simulation technique for systems such as the suspension of solid particles or a polymeric liquid. LBM was first developed by McNamara and Zanetti [15] in 1998 to solve the problems with the lattice gas automata method. Unlike conventional numerical schemes based on the discretization of macroscopic continuum equations, the LBM is based on microscopic models and mesoscopic kinetic equations. LBM recovers the N-S using Chapman-Enskog expansion. One of the most important benefits of lattice Boltzmann is the explicit form of governing equation and an easy solution to parallel equations and boundary conditions employment on the curved boundaries. The lattice Boltzmann is usually applicable to the fields of incompressible flow simulation in complex geometries like blood flow in vessels, multiphase flows, free convection problems, moving boundaries, chemical reactions, porous media flows, suspended particles, MHD flows, non-Newtonian fluid flows, large eddy simulations, turbulence flows in aerodynamics, and other applications [16,17]. It was also developed into an efficient method for solving the problems including the interaction of flow and solid [18,19]. Cheng and Zhang [19] proposed a proper model to simulate the fast boundary movements and a high-pressure gradient occurring in the fluid-solid interaction. In their research, mitral valve jet flow considering the interaction of leaflets and fluid has been simulated.

Applications in a multitude of fields such as drug delivery in medicine or solid-liquid separation in process engineering rely on the physical laws of particulate flows. Often, a raw approximation suffices to design facilities; however, a more in-depth understanding of the dynamics and impact of the acting forces is crucial in the process of improvement [20].

Therefore, they have provided a reasonable basis for simulating a large number of particles, which is computationally expensive. Due to the advances in computing architecture and algorithms in recent years, it is possible to simulate a large number of single particles [21]. Such Euler-Lagrange approaches have become a feasible approach since they are based on simple differential equations; therefore, fast computations can be achieved for the purpose of reduced complexity. In such Discrete Element Methods (DEM), the particles can be approximated as spheres in the first step, yielding good accuracy for many applications [22].

Cardiovascular diseases, including stroke, are one of the most common and prevalent causes of human death on the planet. So far, these problems have been experimentally and theoretically studied. In the field of numerical analysis, further research has been directed at the recognition of blood properties, and the main vessel geometry has not been comprehensively analyzed so far. Therefore, in this article, the flow of blood fluid in a vessel has been studied. Blood has been considered as a non-Newtonian fluid and simulated using Carreau-Yasuda model. The LBM has been used for obtaining the numerical solution of the flow.

2. Governing equations

LBM has received great attention in recent decades.

This is a reliable and alternative method to CFD and has been successfully used so far in most of the engineering applications such as solving incompressible flows, the flow inside the porous surfaces, multi-phase flows, and the simulation of blood flow [23]. Unlike other methods that consider fluid as continuous, it is considered here as composed of particles. Therefore, LBM is able to model the relationship between the particles, which is the basis of the multi-phase flows. When the Mach number (the ratio of the average velocity of the fluid to the velocity of sound) and Knudsen number (the ratio of the mean free path to the characteristic length of the flow) are small enough, the Boltzmann equations will provide a suitable approximation of Navier-Stokes equations. The final form of Navier-Stokes equations will be Eqs. (1) and (2):

$$\nabla \cdot \vec{u} = 0, \tag{1}$$

$$\rho\left(\frac{\partial \vec{u}}{\partial t} + \vec{u}\cdot\nabla\vec{u}\right) = -\nabla p + \nu\nabla^2\vec{u}, \tag{2}$$

where ρ and ν are the mass density and dynamic viscosity of the fluid, respectively. In addition, $\vec{u} = (u, v)$ and p are the velocity field and pressure, respectively, and t indicates the time. As mentioned before, in LBM, the fluid is composed of given particles, which can collide with each other. In the above method, in addition to the spatial position, velocity is discretized, too. It is shown that the particles move only in the directions that are identified with discrete velocities. The form of the discrete equations of lattice Boltzmann, resulting in the same Navier-Stokes equations (1) and (2) by using the expansion of Chapman-Enskog, is given as follows:

$$f_i(\vec{x}+\hat{e}_i\Delta t, t+\Delta t) - f_i(\vec{x}, t) = -\frac{f_i(\vec{x}, t) - f_i^{eq}(\vec{x}, t)}{\tau}, \tag{3}$$

where $f_i(\vec{x}, t)$ is the distribution function of the particles with velocity $\hat{e}_i$, which is at position $\vec{x}$ at time t. Δt is the time step, $f_i^{eq}(\vec{x}, t)$ is the equilibrium distribution function, and τ indicates the dimensionless relaxation time in the Boltzmann equation. In this work, the LBM with a two-dimensional model of D2Q9 has been used; in addition, as evident in Figure 1, eight moving particles with one fixed particle are used in this model. The velocities of these particles can be written as follows:

$$\hat{e}_i = \begin{cases} (i, i); & i = 0 \\ \left(\cos\frac{\pi(i-1)}{2}, \quad \sin\frac{\pi(i-1)}{2}\right)c; & i = 1-4 \\ \sqrt{2}\left(\cos\frac{\pi(i-9/2)}{2}, \quad \sin\frac{\pi(i-9/2)}{2}\right)c; & i = 5-8 \end{cases} \tag{4}$$

where $c = \Delta x/\Delta t$, and Δx is the distance between two adjacent nodes in the Eulerian grid. The equilibrium distribution function is written as follows:

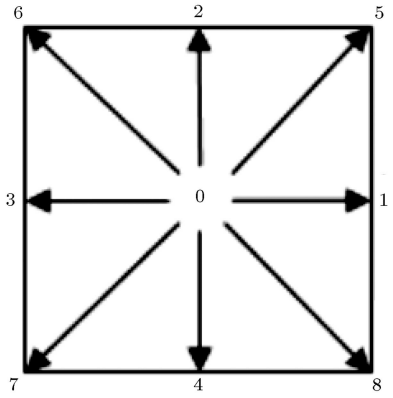

Figure 1. Velocities in the model of D2Q9.

$$f_i^{eq} = w_i\rho\left[1 + 3\frac{(\hat{e}_i\cdot\vec{u})}{c^2} + \frac{9}{2}\frac{(\hat{e}_i\cdot\vec{u})^2}{c^4} - \frac{3}{2}\frac{|\vec{u}|^2}{c^2}\right], \tag{5}$$

where w_i represents the weight coefficients given below:

$$\begin{cases} w_0 = 4/9 \\ w_i = 1/9 \quad \text{if} \quad i = 1-4 \\ w_i = 1/36 \quad \text{if} \quad i = 5-8 \end{cases} \tag{6}$$

On the other hand, the elastic force in the lattice Boltzmann equation is defined as in Eq. (7):

$$F_i = \left(1 - \frac{1}{2\tau}\right) w_i\left[\frac{3(\hat{e}_i - \vec{u})}{c^2} + \frac{9(\hat{e}_i\cdot\vec{u})}{c^4}\hat{e}_i\right]. \tag{7}$$

The kinematics viscosity of the lattice, ν, in the model of D2Q9 is related to the dimensionless relaxation time as follows:

$$\nu = c_s^2\left(\tau - \frac{1}{2}\right). \tag{8}$$

The macroscopic fluid density is obtained through Eq. (9):

$$\rho = \sum_{i=0}^{8} f_i. \tag{9}$$

Moreover, the macroscopic velocity will be:

$$\vec{u} = \frac{1}{\rho}\left[\sum_{i=0}^{8} f_i\hat{e}_i\right]. \tag{10}$$

It is worth mentioning that although the incompressible isotherm flows are simulated in LBM, density is not constant. In addition, pressure does not appear clearly in any of the above equation. In this method, the following equation is used to calculate pressure:

$$p = \rho c_s^2, \tag{11}$$

where p is the unit pressure in the lattice, $c_s = c/\sqrt{3}$ is the sound velocity in lattice, and ρ is the lattice density. In LBM, $\Delta x = \Delta t = 1$ and, therefore, $c_s = 1/\sqrt{3}$. Moreover, the relation between the physical pressure, p_p, and the network pressure, p, is given as in Eq. (12):

$$p_p = \rho_p c_{s,p}^2 = \rho_p \left[c_s^2 \left(\frac{\Delta x_p}{\Delta t_p} \right) \right]^2 = \rho_p \left(\frac{\Delta x_p}{\Delta t_p} \right)^2 \frac{p}{\rho}, \quad (12)$$

where the index p represents the physical quality.

The relationship between tension and the shear rate in Newtonian fluids is linear in form, while, for non-Newtonian fluids, this relationship is non-linear. For non-Newtonian fluids, viscosity depends on shear rate, which is mentioned by different models known as non-Newtonian models. One of the non-Newtonian models used for modeling viscosity is the Carreau-Yasuda model, which is given in Eq. (13) and is usually used to show the exact shear behavior of blood:

$$\frac{\eta - \eta_\infty}{\eta_0 - \eta_\infty} = \left[1 + (\lambda \dot{\gamma})^a \right]^{(n-1)/a}, \quad (13)$$

where η_0 is the viscosity in the zero-shear rate, and η_∞ is viscosity in infinite shear rate. Moreover, λ, n, and a are the time constant, power-law power, and dimensionless parameter, respectively. Herein, a describes the width of the transition area between the zero-shear rate and the power-law areas. The inverse of λ represents the critical shear rate in which viscosity starts to decrease with an increase in shear rate. In Carreau-Yasuda model for shear rates larger than 10^4, viscosity, η_∞, is constant [20]. The shear rate for non-Newtonian models is obtained as follows:

$$S_{\alpha\beta} = \frac{1}{2} \left(\frac{\partial u_\beta}{\partial x_\alpha} + \frac{\partial u_\alpha}{\partial x_\beta} \right), \quad (14)$$

$$D_{II} = \sum_{\alpha,\beta=1}^{l} S_{\alpha\beta} S_{\alpha\beta}, \quad (15)$$

$$\dot{\gamma} = \sqrt{2 D_{II}}, \quad (16)$$

where S is the strain rate tensor, u is the local velocity component of the fluid, D_{II} is the second invariant of the strain rate tensor, and $\dot{\gamma}$ is the shear rate. When the superficial viscosity is known, the instantaneous and local relaxation times for all the walls can be determined, and the changes in distribution functions can be obtained according to Eq. (3).

The non-Newtonian blood flow in the present manuscript has been considered as a laminar, incompressible and steady flow with an approximate Mach number less than one. The solution is obtained using the LBM. The lattice Reynolds number is defined as $\mathrm{Re}_{lbm} = \frac{u_{lbm} D}{v_{lbm}}$. Table 1 summarizes the coefficients of the Carreau-Yasuda model.

Table 1. Coefficients of Carreau-Yasuda model [24].

η_0	η_∞	λ	a	n
0.056	0.005	3.131	2	0.4

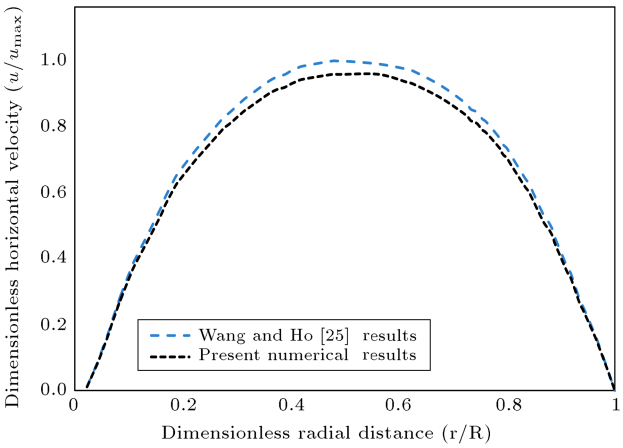

Figure 2. Comparison of outlet velocity between the present results and Wang and Ho [25] results.

3. Verification

To verify the present results based on those related to non-Newtonian Carreau-Yasuda fluid flow, the velocity profile at the channel outlet has been compared with the results of Wang and Ho [25] with a 30×100 grid. The parameters of the Carreau-Yasuda model are chosen as those used in [25], presented in Table 1. Knowing τ, we can obtain viscosity in the zero shear rate η_0 and with the Reynolds number 1.1 for the grid; the numerical value of inlet velocity can be calculated. By calculating the numerical value of $\frac{u}{u_{\max}}$, the horizontal velocity profile at the outlet of the canal is depicted in Figure 2. It is observed that there is very good agreement between the present results and those obtained in [25]. According to Figure 2, the maximum velocity at the center of both diagrams tends to be of the same value; therefore, the veracity of the obtained results for the two-dimensional channel of the present problem can be understood for other simulations in this research.

4. Investigation of blood flow in an open straight vessel

4.1. Effect of Reynolds number

Reynolds number is used to determine the velocity of flow. This study takes into account the Reynolds number from 0.05 to 1.5 to carry out numerical computation in order to find the effect of oscillatory flow inside the vessel. Figure 3 shows that an increase in Re from 0.05 to 1.5 increases the axial velocity of blood with time. Large Re (= 1.5) results in the thinner concentrated boundary layer on the surface, while low Re (= 0.05)

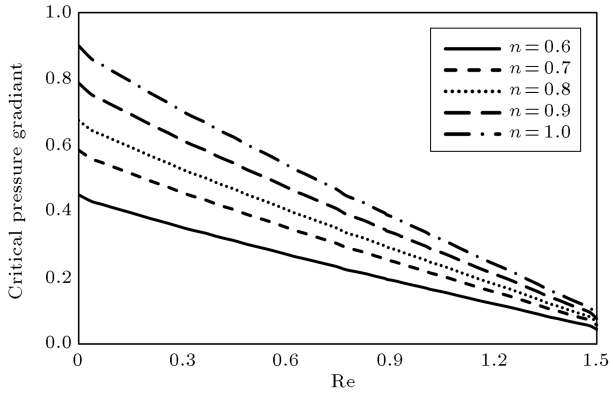

Figure 3. Variation of critical pressure gradient versus Reynolds numbers for different power-law indexes.

causes high concentration on surface and velocity of blood tends to zero. By increasing power-law index, the flow shows higher Reynolds number; hence, the value of local shear rate will increase, which causes a decrease in viscosity and an increase in Reynolds number as a result.

4.2. The effect of the vessel diameter and blood viscosity on the blood flow

Clearly, the application of the Computational Fluid Dynamics (CFD) technique reduces the complexity and cost of empirical works [26]. Resistance is basically in the form of friction. Since, in fact, the friction between blood and the walls of vessels develops resistance against blood flow. Such resistance depends upon the length of the vessel, vessel diameter, and blood viscosity. In this study, the effects of vessel diameter and blood viscosity on the resistance against blood flow are studied.

By inserting factors influential in resistance into the previous formula, another formula titled "the Poiseuille law" can be obtained as follows:

$$Q = P \times D^4/(\mu \times L), \tag{17}$$

where Q, P, D, and L are blood flow rate, pressure, vessel diameter, viscosity, and vessel length, respectively.

This formula indicates the ability of blood to flow in any assumed vessel. According to the formula, the amount of blood flow has a direct relationship with the pressure difference between the two ends of the vessel. In addition, it has a direct relationship with the fourth power of vessel diameter and an inverse relationship with the length of vessel and blood viscosity.

Figure 4 displays the variation of the dimensionless flow rate for different vessel diameters. As is known, the blood present in a vessel is almost motionless near the walls of the vessel. For this reason, the velocity of blood flow at the center of vessels would be very high, while it would have very low velocity near the walls. In addition, according to the obtained results shown in Figure 4, an increase in the diameter

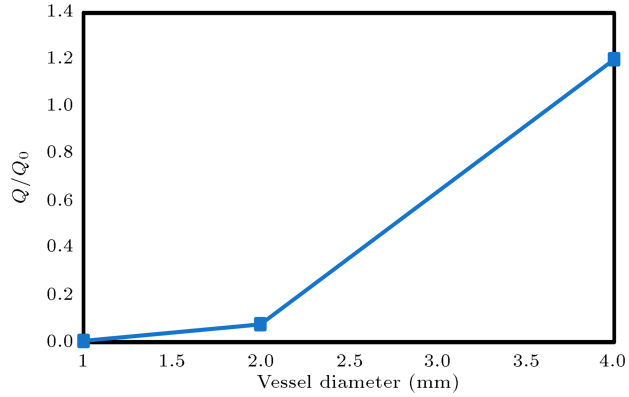

Figure 4. The effect of vessel diameter on blood flow.

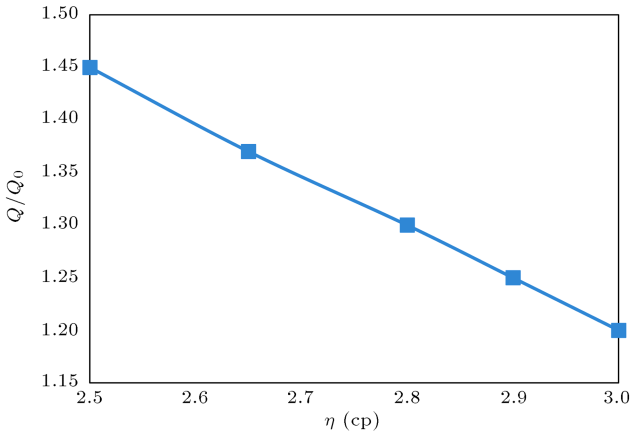

Figure 5. The effect of viscosity on the blood flow rate.

of the vessels leads to an increase in the velocity of blood flow in the center. For that reason, the amount of blood transmitted through a vessel would increase as a result of an increase in the diameter of the vessel. In fact, if all other factors are kept constant, the amount of blood transmitted through a vessel would correlate with the fourth power of the vessel diameter. Thus, in Figure 4, three vessels are investigated that are of a similar length, but differing diameters (1, 2, and 4 mm). It should be pointed out that even such small differences in the diameter of vessels can result in a 256-time increase in the amount of blood transmitted through a vessel.

Figure 5 displays the variation of the dimensionless flow rate for different viscosities. In this figure, the variation of three values of viscosities is illustrated while being transmitted in a vessel with a constant diameter. Because the blood velocity in the small vessels is extremely low and often less than 1 mm/s, the blood viscosity can be as high as ten times. Increasing the viscosity of blood is a sign of a disease called sickle cell anemia, in which red blood cells become sickle cell and rigid. Thus, blood flow in the cells of people suffering from anemia is very fast, while the speed of blood flow in patients having polycythemia is very slow. In patients having anemia, the concentration of

red blood cells is very low, while it is very high in those having polycythemia. Therefore, because of their malformation, they lose the ability to carry oxygen [27].

As is known, greater friction would occur near the vessel walls because of the high viscosity of the liquid flowing within a vessel, leading to greater resistance. Such an effect is illustrated in Figure 5. In all of the cases, the amount of pressure required to drive the liquids forward in the vessel is equal together. However, since the three liquids have differing viscosities, the blood flow is different from each other. The major factor contributing to the creation of blood viscosity is the concentration of red blood cells.

The previous pieces of research illustrate that viscosity in blood is three times that of water [28]. Nevertheless, if the concentration of red blood cells is reduced to half of its natural amount, viscosity in blood is twice that of water. In addition, if the concentration of red blood cells doubles in amount, the viscosity of blood is 15 times that of water.

From the discussion above, it could be concluded that pressure and resistance have two opposing effects on blood flow. In other words, pressure tends to increase the flow, while resistance tends to decrease it. This phenomenon is shown with the following formula:

$$\text{Blood flow} = \text{pressure/resistance}.$$

The above formulas have played a key role in almost all of the studies on the hemodynamics of systemic circulation and, consequently, they have to be understood thoroughly before any attempt to be made at interpretations regarding blood flow. Resistance is equal to the difference in pressure divided by the blood flow. Thus, for constant blood flow, an increase in pressure will increase the resistance. Nevertheless, since the viscosity of blood is directly proportional to resistance, it is inversely proportional to the blood flow. Thus, if viscosity increases, it will increase resistance and decrease blood flow.

5. Results of closed ends coronary bifurcation

5.1. Problem modeling

The geometry of coronary bifurcation is shown in Figure 6. Considering the grid independence, the number of elements is considered as 11000 to simulate the blood flow in the present study.

5.2. Assumptions and boundary conditions of the present problem

Simulation and problem solving have been done with the following assumptions:

I. The walls of the vessel are assumed to be rigid;

II. The problem is solved in the unsteady state;

III. The blood flow is considered incompressible;

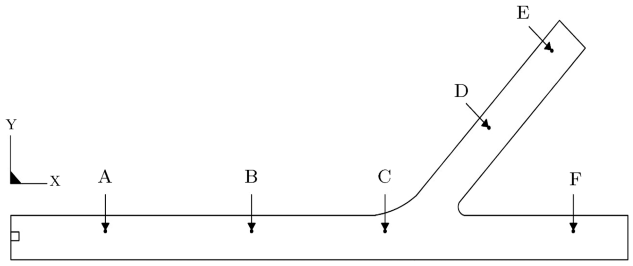

Figure 6. Display of the coronary bifurcation geometry modeled in this study.

The boundary conditions are also considered as follows:

I. The end of the vessel is closed (no-slip boundary condition is used);

II. The motion of all wall grids is bounded in all directions, or the no-slip condition is used (speed in the walls is assumed zero).

5.3. Pressure distribution of blood in different points of the coronary bifurcation

The total amount of time to carry out the analysis is 2 seconds. However, the results of analysis indicate that the blood flow hits the end of the blocked vessel and is reflected by no more than 2 seconds. The histories of pressure changes in different parts of the vessel are shown in Figure 7 with regard to the points indicated in Figure 6. Due to the passage of blood from one point, a peak appears in the pressure diagrams. The peaks at points A and B are related to the passage of high-pressure blood flow. The values of pressures are 0.0664 and 0.0279 for points A and B, respectively. This indicates that blood pressure is damping in the intravascular motion. Two peaks are observed in the pressure history of point C, which is near the junction of the vessel. The first peak is associated with the initial flow of blood, and the second peak represents the secondary and reflected flow from the end wall

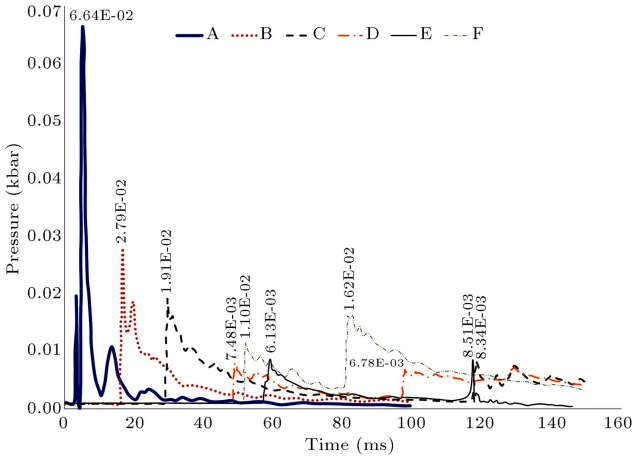

Figure 7. History of pressure at points A, B, C, D, E, and F.

of branches. At point C, the main and return flows of blood make the maximum pressure of 0.0191 and 0.00834, respectively. The graph of point D, which is located in the subbranch, is also the same, and the mainstream makes a pressure rate of 0.00748. At point F, which is located along the main branch, the maximum pressure due to the main blood flow and the reflection of blood flow through that peak point will be 0.0011 and 0.00162, respectively. The most important point in the present analysis is to estimate the pressure caused by blockage of the vessel in the desired location of point E, which, according to the pressure history of that point, the maximum pressure due to the passage of blood at the end of the branch is 0.00851.

Of note, blood flows through the vessel and is reflected when it reaches the closed E point. The amount of reflection pressure based on the type and angle of the collision is several times greater than the blood pressure before the collision. For this reason, the amount of pressure on point E is far greater than the pressure before it hits point E. The simulation results include time pressure contours and pressure diagrams. It should be noted that, in all diagrams and contours, the pressure is in terms of time and time in seconds.

5.4. Analysis of the blood flow inside the coronary bifurcation according to the behavior of pressure contours

As can be seen below, pressure contours are formed from the entrance and expand at approximately the same point with the release of blood in the vessel, which can be concluded from changes in blood pressure throughout the coronary and blood flow patterns at different times shown in the diagrams and figures below.

Figure 8 shows that the blood flow throughout the coronary bifurcation is as expected. Nevertheless, while moving along the way, the pressure decreases and the blood moves to the two ways.

According to the pressure contours in Figure 9, that part of blood flow that passes through the straight line is subject to higher pressure compared to the flow that enters the subbranch. It can be analyzed in such a way that the motion of blood in the previous direction is more significant, and the blood flow tends to move at the highest levels of irregularities and the lowest levels of energy [29]. Therefore, a large part of the blood enters into a direct and high-pressure branch. In addition, according to the pressure contours created in the main and secondary branches of Figure 10, it can be seen that the blood flow in the branch is accompanied by lower pressure changes and is less turbulent than the main branch flow due to the high speed and pressure in this branch.

In Figure 11, both blood flows start with almost identical pressure profiles from the end of the path.

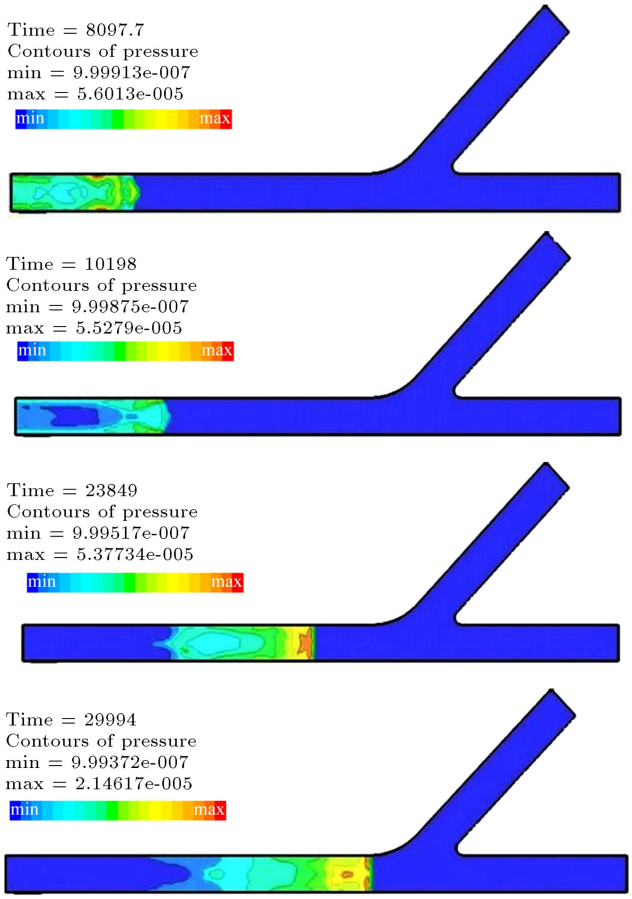

Figure 8. Motion of blood flow in two ways.

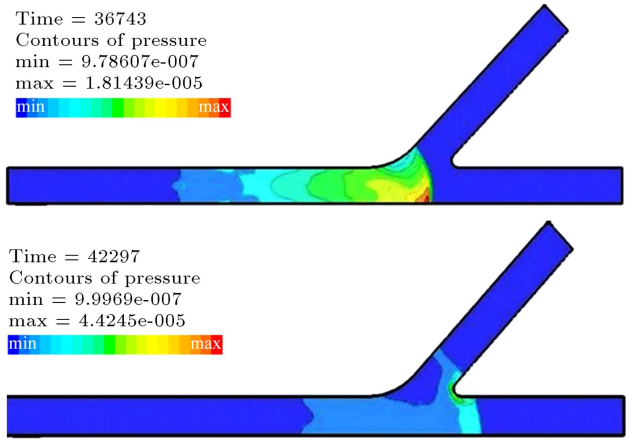

Figure 9. The blood flow and its collision into two ways.

However, in the return path, the blood flow pressure in the main branch is higher than the subbranch. The blood flow of the main branch reaches the intersection of the vessel firstly. Moreover, because of the low pressure of the subbranch, it enters this branch and does not enter the main path at all. Then, by moving the blood flow of the subbranch and colliding it with the main branch of the pressure contour, they are combined and move towards the low-pressure intersection of the

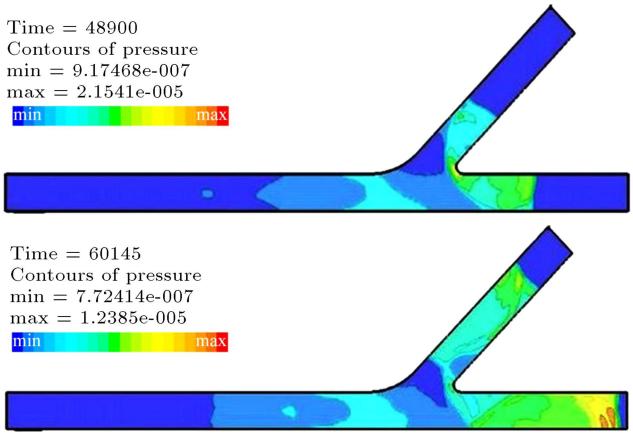

Figure 10. Crossing the blood flow in two ways and its reflection through the walls.

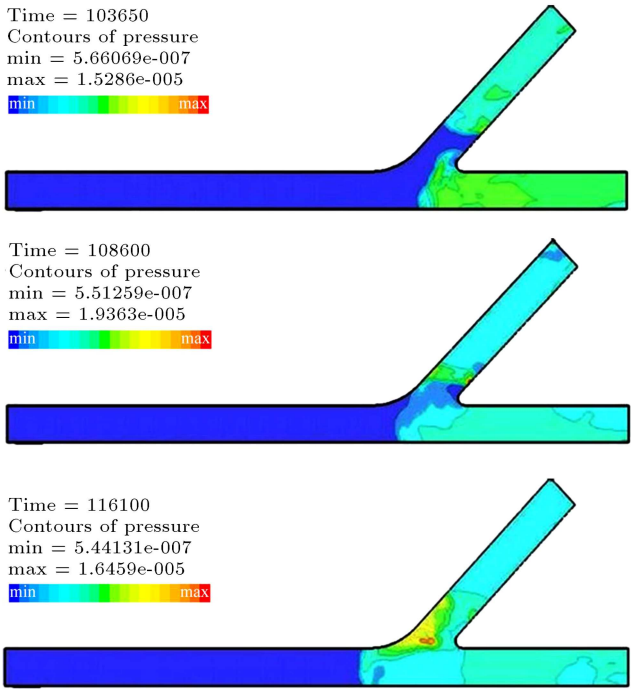

Figure 11. Bringing the reflected blood flow together in a two-way and forming a single flow.

coronary bifurcation. As can be seen, the pressure at this point will be at the highest level. Then, after moving the blood from the intersection of the branches, with the profile of the pressure, it almost uniformly moves to the beginning of the path.

6. Conclusion

This study modeled the blood flow in a straight vessel and coronary bifurcation with a constant velocity flow input and showed computational results together with fluid flow inside the human vessel using by LBM. Then, this paper investigated the effect of Reynolds number and the effect of the vessel diameter and blood viscosity on the blood flow. Now, the concluding remarks are presented in the following:

- The results were compared with the available numerical outputs, and this comparison showed considerable agreement between them;
- Non-Newtonian LBM showed its high ability in the modeling of rheological problems;
- Large Reynolds number resulted in thinner concentration boundary layer on the surface, while low Reynolds number caused high concentration on surface and the velocity of blood tended to zero;
- An increase in the diameter of the vessels would increase the velocity of blood flow in the center;
- Increasing the viscosity of the blood flowing within a vessel increased the friction at the vessel walls and, as a result, the higher resistance was observed;
- Pressure and resistance had two opposing effects on blood flow. In other words, pressure tended to increase the flow, while resistance tended to decrease it;
- The amount of blood flow had a direct relationship with the pressure difference between the two ends of the vessel. In addition, it had a direct relationship with the fourth power of vessel diameter and an inverse relationship with the length of vessel and blood viscosity;
- As the blood released in the coronary bifurcation, pressure contours formed from the entrance and expanded at approximately the same point;
- The obtained results showed that part of the blood flow passing through the straight line had higher pressure than the flow that entered the subbranch;
- The blood flow in the subbranch was accompanied by lower pressure changes and was less turbulent than the main branch flow;
- In the return path, the blood flow pressure in the main branch was higher than that in the subbranch. The blood flow of the main branch reached the intersection of the vessel first.

One of the applications of this research can help recognize and treat vascular diseases including obstruction. As is known, a progressive decrease in the diameter of the vessels can lower the blood flow to the heart and may cause blockage of one or more vessels. In all old people, the disease develops with varying degrees of intensity and gradually reduces the progression of the coronary reserve.

References

1. DiVito, K.A., Daniele, M.A., Roberts, S.A., Ligler, F.S., and Adams, A.A. "Microfabricated blood vessels

undergo neoangiogenesis", *Data in Brief*, **14**, pp. 156-162 (2017).

2. Moccia, S., De Momi, E., El Hadji, S., and Mattos, L.S. "Blood vessel segmentation algorithms-review of methods, datasets and evaluation metrics", *Comp. Meth. and Prog. in Biomed.*, **158**, pp. 71-91 (2018).
3. Fedosov, D.A., Caswell, B., Suresh, S., and Karniadakis, G.E. "Quantifying the biophysical characteristics of Plasmodium-falciparum-parasitized red blood cells in microcirculation", *Proc. Nat. Acad. Sci.*, **108**(1), pp. 35-39 (2011).
4. Wu, J., Hu, Q., and Ma, X. "Comparative study of surface modeling methods for vascular structures", *Comp. Med. Imaging Graph.*, **37**(1), pp. 4-14 (2013).
5. Campochiaro, P.A. "Molecular pathogenesis of retinal and choroidal vascular diseases", *Prog. Retin. Eye Res.*, **49**, pp. 67-81 (2015).
6. De Momi, E., Caborni, C., Cardinale, F., Casaceli, G., Castana, L., Cossu, M., Mai, R., Gozzo, F., Francione, S., and Tassi, L. "Multi-trajectories automatic planner for Stereo Electro Encephalo Graphy (SEEG)", *Int. J. Comput. Assist. Radiol. Surg.*, **9**(6), pp. 1087-1097 (2014).
7. Essert, C., Fernandez-Vidal, S., Capobianco, A., Haegelen, C., Karachi, C., Bardinet, E., Marchal, M., and Jannin, P. "Statistical study of parameters for deep brain stimulation automatic preoperative planning of electrodes trajectories", *Int. J. Comput. Assist. Radiol. Surg.*, **10**(12), pp. 1973-1983 (2015).
8. Navidbakhsh, M. and Rezazadeh, M. "An immersed boundary-lattice Boltzmann model for simulation of malaria-infected red blood cell in micro-channel", *Scientia Iranica*, **19**(5), pp. 1329-1336 (2012).
9. Faria, C., Sadowsky, O., Bicho, E., Ferrigno, G., Joskowicz, L., Shoham, M., Vivanti, R., and De Momi, E. "Validation of a stereo camera system to quantify brain deformation due to breathing and pulsatility", *Med. Phys.*, **41**(11), p. 113502 (2014).
10. Cardinale, F., Pero, G., Quilici, L., Piano, M., Colombo, P., Moscato, A., Castana, L., Casaceli, G., Fuschillo, D., and Gennari, L. "Cerebral angiography for multimodal surgical planning in epilepsy surgery: description of a new three-dimensional technique and literature review", *World Neurosurg*, **84**(2), pp. 358-367 (2015).
11. Alishahi, M., Alishahi, M.M., and Emdad, H. "Numerical simulation of blood flow in a flexible stenosed abdominal real aorta", *Scientia Iranica*, **18**(6), pp. 1297-1305 (2011).
12. Hernández-Pérez, M., Puig, J., Blasco, G., de la Ossa, N.P., Dorado, L., Dávalos, A., and Munuera, J. "Dynamic magnetic resonance angiography provides collateral circulation and hemodynamic information in acute ischemic stroke", *Stroke*, **47**(2), pp. 531-534 (2016).
13. Rochitte, C.E., George, R.T., Chen, M.Y., Arbab-Zadeh, A., Dewey, M., Miller, J.M., Niinuma, H., Yoshioka, K., Kitagawa, K., and Nakamori, S. "Computed tomography angiography and perfusion to assess coronary artery stenosis causing perfusion defects by single photon emission computed tomography: the CORE320 study", *Eur. Heart J.*, **35**(17), pp. 1120-1130 (2014).
14. Pamme, N. "Continuous flow separations in micro fluidic devices", *Lab on a Chip*, **7**, pp. 1644-1659 (2007).
15. McNamara, G. and Zanetti, G. "Use of the Boltzmann equation to simulate lattice gas automata", *Physics of Review Letters*, **61**(5), pp. 23-32 (1998).
16. Chen, S. and Doolen, G.D. "Lattice Boltzmann method for fluid flows", *Ann. Rev. of Fluid Mech.*, **30**(1), pp. 329-364 (1998).
17. Succi, S. *The Lattice Boltzmann Equation for Fluid Dynamics and Beyond*, Oxford University Press: Oxford (2001).
18. Wang, H., Cater, J., Liu, H., Ding, X., and Huang, W. "A lattice Boltzmann model for solute transport in open channel flow", *J. of Hydrology*, **556**, pp. 419-426 (2018).
19. Cheng, Y. and Zhang, H. "Immersed boundary method and lattice Boltzmann method coupled FSI simulation of mitral leaflet flow", *Comp. and Fluids*, **39**(5), pp. 871-881 (2010).
20. Lecrivain, G., Rayan, R., Hurtado, A., and Hampel, U. "Using quasi-DNS to investigate the deposition of elongated aerosol particles in a wavy channel flow", *Comp. and Fluids*, **124**, pp. 78-85 (2016).
21. Vi, A., Pouransari, H., Zamansky, R., and Mani, A. "Particle-laden flows forced by the disperse phase: Comparison between lagrangian and eulerian simulations", *Int. J. of Multiphase Flow*, **79**, pp. 144-158 (2016).
22. Henn, T., Thäter, G., Dörfler, W., Nirschl, H., and Krause, M.J. "Parallel dilute particulate flow simulations in the human nasal cavity", *Comp. and Fluids*, **124**, pp. 197-207 (2016).
23. Wu, J. and Shu, C. "An improved immersed boundary-lattice Boltzmann method for simulating three-dimensional incompressible flows", *J. of Comput. Phys.*, **229**, pp. 5022-5042 (2010).
24. Carreau, P.J. "Rhology equations from molecular network theories", *J. of Rheo.*, **16**(1), p. 127 (1972).
25. Wang, C.H. and Ho, J.R. "A lattice Boltzmann approach for the non- newtonian effect in the blood flow", *Comput. Math. Appl.*, **62**, pp. 75-86 (2011).
26. Khodayari Bavil, A. and Razavi, S.E. "On the thermo flow behavior in a rectangular channel with skewed circular ribs", *Mech. & Ind.*, **18**(2), p. 225 (2017).
27. Bagchi, P. "Mesoscale simulation of blood flow in small vessels", *Biophys. J.*, **92**, pp. 858-1877 (2007).
28. De Hart, J., Baaijens, F.P.T., Peters, G.W.M., and Schreurs P.J.G. "A computational fluid-structure interaction analysis of a fiber-reinforced stentless aortic valve", *J. of Biomech.*, **36**, pp. 699-712 (2003).

29. Arokiaraj, M.C., De Santis, G., De Beule, M., and Palacios, I.F. "A novel tram stent method in the treatment of coronary bifurcation lesions - finite element study", *PLoS ONE*, **11**, e0149838 (2016).

Biographies

Hamed Akhtari Shishavan was born in 1984 in Iran. He received BS degree in Mechanical Engineering from Islamic Azad University of Kerman in 2005. He received MSc degree in Mechanical Engineering (energy conversion field) from Islamic Azad University of Takestan in Iran. Currently he is a PhD student in Urmia university. He has been also an Academic Member in Islamic Azad University of Miandoab since 2011. His main research favorites include CFD, energy conversion, Lattice Boltzmann, and biomechanics problems.

Iraj Mirzaee was born in 1960 at Ahar city of Iran. He received BS degree in Mechanical Engineering from Mashhad University in 1986. He started MSc degree in Mechanical Engineering (energy conversion field) in Esfahan University of Technology in Iran and, finally, he received his PhD in Mechanical Engineering (energy conversion field) in 1997 at the Bath University in England. He is a Professor at the Mechanical Engineering Department at Faculty of Engineering of Urmia University. His professional interests are in the field of CFD, turbulent fluid flow, energy conversion problems, and gas turbine.

Nader Pourmahmoud was born in 1969 in Iran. He received his BS degree in Mechanical Engineering from Shiraz University in 1992. After achieving some practical engineering projects till 1997, he started his MSc degree in Mechanical Engineering (energy conversion field) in Tarbiat Modarres University in Tehran, Iran; finally, he received his PhD degree in Mechanical Engineering (energy conversion field) in 2003 at the same university. He has joined the Faculty of Engineering of Urmia University since 2003, where he is a Professor in the Mechanical Engineering Department. His professional interest is in the field of CFD of Turbulent fluid flow, energy conversion problems especially in the vortex tube, and lattice Boltzmann method.